American Journal of Environmental Sciences

Original Research Paper

Transverse Bed-Slope, Lateral Bed-Load Rate and Bed-Load Deviation Angle in Meandering Alluvial Streams

Youssef Ismail Hafez

Independent Researcher, Egypt

Article history
Received: 15-05-2024
Revised: 29-07-2024
Accepted: 03-08-2024

Email: youssefhafez995@gmail.com

Abstract: A novel expression for the deviation angle of the bed-load discharge is developed which allows its distinction with the other deviation angles of the flow velocity and boundary shear stress. A transverse bed-slope equation is developed which compares very well with experimental data and field data at the Fall River and Muddy Creek, USA. Stream-wise computations are successfully performed of the transverse bed slopes in the Fall River. Correction for the thickness of the bed-load layer in curved channels and expression for the lateral distribution of grain sizes are presented. A contribution is made in developing the upslope lateral bed-load transport rate equation which allows modification of well-known existing transverse bedload rate equations. An expression of the stream-wise bed-load transport in curved and meandering channels is proposed. The developed approach equations have a higher degree of physical realism than existing methods.

Keywords: Meandering Open Channels, Transverse Bed Slope, Deviation Angle of The Bed-Load, Lateral Bed Load Transport Rate, Stream-Wise Bed-Load Transport in Curved Channels

Introduction

There is a close interrelationship between river flow, sediment transport, and river channel formation, (Chang 1992; Da Silva, 2006; Ferreira da Silva and Ebrahimi; 2017; Weiss and Higdon, 2022). In other words, meander planform, bed topography, bank erosion, and lateral migration, are very much related to the dynamics of flow and sediment transport in curved channels, which, in turn, provides the basis for analysis and modeling, (Chang, 1992). Hafez (2022) addressed the importance of the water flow discharge and sediment load as the driving mechanisms for forming and influencing alluvial river meander plan forms. “The role of secondary currents in curved alluvial channels consists of moving sediment particles away from the concave bank and toward the convex bank. This general movement has effects on point-bar formation, sediment sorting, lateral migration, bank erosion, and width variation. At the time of transverse equilibrium, the lateral bed-load transport is counterbalanced by the transverse bed slope”, (Chang, 1992). In spite of such important statements, works on lateral sediment transport rate and its associated transverse bed slope and processes date back to the last century (e.g., Ikeda (1982); Parker (1984); Falcon-Ascanio and Kennedy (1983); Odgaard (1986a-b)).

Understanding the mechanics of flow and sediment is a necessary part in order to understand the meandering phenomenon. Recent investigation of the mechanics of flow in meandering channels is addressed by Hafez (2024); while the mechanics of sediment transport in alluvial meandering channels is addressed herein.

In spite of numerous studies on flow and sediment transport mechanics of river meandering, in spite of the advancement of computer power to perform two and three-dimensional detailed computations and in spite of advances in measurement techniques, still several fundamental issues of the mechanics of flow and sediment transport in meandering channels have not been solved even on the scale of the one-dimensional analysis, (Hafez, 2024). On the other hand, experimental and field works unfortunately have not often tried to measure the transverse bed load rate as in the following two examples. In the experiments of He *et al*. (2021) in two laboratorial sine-generated channels, i.e., one with a deflection angle = 30° and the other 110°, the longitudinal and transverse transport of bedload were evaluated in the examined bends of the two meandering flumes, however, they were expressed in the unit of volume (m^3) which precludes knowing the actual rate of bed-load transport. Intensive field data collection of 1499 bends was performed by Zhou and Tang (2022)

using Landsat images in the Yimin River China, however, no hydraulic and sediment data were collected.

In this study, several fundamental issues in sediment transport mechanics in alluvial meandering rivers such as the transverse bed slope, the transverse bed load rate, the thickness of the bed load layer in alluvial meandering channels, and the transverse bed load deviation angle are re-visited and new developments are presented.

Some assumptions in past studies have been made which are liable for improvements as seen in the next review section. In this study, some of the fundamental assumptions in the pioneering works are revisited and modified. In addition, equations are presented in attractable and user-friendly forms which allow their inclusion in analytical and numerical models. Mechanics of sediment in curved channels in this study include mainly the transverse bed slope, the lateral bed-load transport, and bed-load deviation angle in addition to longitudinal bed load in curved channels.

Review of Curved Channel Mechanics

In a theoretical approach for determining the transverse bed slope in curved channels, Ascanio and Kennedy (1983) balanced the radial component of the fluid force shear stress (τ_{or}) by the submerged weight component of the bed layer down the transverse bed slope with angle (β), that is:

$$\tau_{or} = z_b\,(1-\lambda)(\rho_s-\rho)\,g\,\sin\beta \tag{1}$$

where, z_b is the thickness of the bed-load layer in straight channels, λ is the bed-layer porosity, ρ_s is the sediment density, ρ is the water density and g is the gravitational acceleration. They used the bed-layer thickness given by Karim (1981) which is expressed as:

$$z_b = d\,\frac{U_*}{U_{*c}} \tag{2}$$

where, $d = d_{50}$ is the median bed material size, $U_* = U/(f/8)^{1/2}$ is the shear velocity, U is the average main velocity, f is the Darcy-Weisbach friction factor and U_{*c} is the critical shear velocity for incipient motion given as:

$$U_{*c} = \left(\frac{\rho_s-\rho}{\rho}\,g\,d\,\tau_{*c}\right)^{1/2} \tag{3}$$

where, τ_{*c} is the critical Shields' stress. To get the lateral bed-shear stress, Ascanio and Kennedy (1983) balanced the moment due to the centrifugal acceleration by that due to the radial bed shear stress and obtained the relation:

$$\tau_{or} = \rho\,D\,\frac{\bar{U}^2}{r}\,\frac{1+m}{(2+m)m} \tag{4}$$

where, D is the local flow depth, $\bar{U}$ is the depth-averaged longitudinal velocity and r is the channel radius of curvature. In the central portion of the channel cross-section in wide channels which is the case herein, $\bar{U}$ could be assumed equal to the cross-sectional-averaged longitudinal velocity. The quantity m is related to the Darcy-Wabash friction factor (f) and the von Karman constant (κ) by:

$$\frac{1}{m} = \frac{1}{\kappa}\sqrt{\frac{f}{8}},\ \text{or}\ m = \kappa\sqrt{\frac{8}{f}} \tag{5}$$

It is noted that Eq. (4) for the lateral bed shear stress neglects the contribution by the transverse pressure force which is induced by the transverse water surface slope in spite that this pressure force is a key part in curved flows as pointed out by Hafez (2024).

Substitution of Eqs. (1-3) into Eq. (1) while β is assumed to be small enough that $\tan\beta \approx \sin\beta$ yields:

$$S_t = \tan\beta = \rho\,D\,\frac{\bar{U}^2}{g\,r}\,\frac{1+m}{(2+m)m}\,\frac{U_{*c}}{(1-\lambda)(\rho_s-\rho)\,d\,U_*} \tag{6}$$

If $\beta = 15°$, $\sin(15°) = 0.259 \approx 0.26$ while $\tan(15°) = 0.268 \approx 0.27$. Therefore, it can be safely stated that when the transverse bed slope is less than 0.25 or its angle $\beta<15°$ the assumption of equality of the sine and tangent functions becomes valid.

Ascanio and Kennedy (1983) actually did not consider Eq. (6) but they obtained a different simplified form by substituting Eqs. (2-4) into Eq. (1) and incorporating the simplified Nunner's relation (Nunner, 1956): $m = 1/f^{1/2}$ to get:

$$S_t = tan\,\beta = \frac{dD}{dr} \cong sin\,\beta = \frac{D}{r}\,F_d\,\frac{(8\,\tau_{*c})^{1/2}}{(1-\lambda)}\,\frac{1+f^{1/2}}{1+2\,f^{1/2}} \tag{7}$$

where, β is assumed to be small enough that $\tan\beta \approx \sin\beta$ and F_d is the densimetric Froude number defined by:

$$F_d = \frac{\bar{U}}{\{[(\rho_s-\rho)/\rho]\,g\,d\}^{1/2}} \tag{8}$$

Equation (7) was found to fit the experiments of Zimmerman and Kennedy (1978) if $\frac{(8\,\tau_{*c})^{1/2}}{(1-\lambda)} = 1.3$. Ascanio and Kennedy (1983) report that for $\tau_{*c} = 0.06$ the resulting porosity is $\lambda = 0.47$, a not-unreasonable value for the agitated moving bedload particles. It should be noted that Yeh and Kennedy (1993) introduced a correction factor, C_b, to extend Eq. (2) to other than the primary-flow direction for which it was derived. Through the calibration process of measured and computed depth profiles, they obtained values for C_b ranging from 0.75-0.45 and stated that it should be dependent on the bed-particle size.

To integrate Eq. (7) to get the transverse bed profile they followed the assumption of Yen and Yen (1971) that:

$$S = S_c\,\frac{r_c}{r} \tag{9}$$

where the subscript c designates the centreline value and *S* is the channel longitudinal slope. Equation (9) is used to express the radial variation of the depth-averaged velocity ($\overline{U}(r)$) as:

$$\overline{U}(r) = \sqrt{\frac{8\ g\ S\ D(r)\delta_\tau(r)}{f}} = \sqrt{8\ g\ S_c\ \frac{r_c}{r}\ \frac{D(r)\delta_\tau(r)}{f}} \quad (10)$$

where, $\delta_\tau(r)$ is the bed shear stress reduction factor due to the bank effect which is unity for very wide channels.

Substituting Eq. (10) into Eq. (7) and integrating the resulting expression for *dD*/*dr* yields:

$$\frac{1}{\sqrt{D}} - \frac{1}{\sqrt{D_c}} = \left[\frac{1}{\sqrt{r}} - \frac{1}{\sqrt{r_c}}\right] \frac{(8\,\tau_{*c})^{1/2}}{(1-\lambda)}\ \frac{1+f^{1/2}}{1+2\,f^{1/2}}\ \left\{\frac{8\ g\ S_c\ r_c \delta_\tau(r)}{f\ g\ [(\rho_s-\rho)/\rho]\ d}\right\}^{1/2} \quad (11)$$

where, D_c is the channel center line depth. Equation (11) was found by Ascanio and Kennedy (1983) to fit well the transverse bed profiles from experiments by Zimmermann (1974) and the Missouri River data by Falcon-Ascanio (1979). It is noted, however, that several assumptions exist in Ascanio and Kennedy (1983) such as the simplified radial bed shear stress in Eq. (4), the use of bed layer thickness from Eq. (2) that does not consider channel curvature and the Nunner's simplification of (m).

Based on the force balance on a sediment particle between the bottom currents and the submerged weight directed down the transverse bed slope, Engelund (1974) derived the following equation:

$$tan\,\delta_{vb} = \frac{tan\,\beta}{tan\,\phi} \quad (12)$$

where, δ_{vb} is the flow velocity deviation angle at the bottom (i.e., tan δ_{vb} = v_b/u_b; v_b and u_b are the bed velocities in the lateral and stream-wise directions, respectively), β is the angle of the transverse bed slope, ϕ is the angle of repose of sediment and tan ϕ is the dynamic friction coefficient.

Bridge (1977) approach on the transverse bed slope, S_t, is based on Eq. (12) and the angle of flow velocity deviation given by Rozovskii (1957) as tan δ_{vb} = 11 (*D*/*r*), which when inserted into Eq. (12) yields:

$$S_t = tan\,\beta = \frac{dD}{dr} = 11\ \frac{D}{r} tan\,\phi \quad (13)$$

Integrating Eq. (13) and evaluating the integration constant at the channel center line yield:

$$\frac{D}{D_c} = \left(\frac{r}{r_c}\right)^{11\tan\phi} \quad (14)$$

To obtain the grain size distribution, Bridge (1977) balanced the transverse drag force on a given particle located on the transverse bed slope and the weight component down the slope as:

$$\pi\left(\frac{d}{2}\right)^2 \tau_{or} = \pi\left(\frac{d}{2}\right)^2 \tau_o \tan\delta_{vb} = \frac{4}{3}\,\pi\left(\frac{d}{2}\right)^3 (\rho_s - \rho)\ g \sin\beta \quad (15)$$

where, τ_o is the longitudinal bed shear stress. It is noted that Eq. (15) is based on the assumption: $\tau_r = \tau_o$ (tan δ_{vb}), which means that the angle between the longitudinal and radial bed shear stress is the same angle between the longitudinal and radial flow velocity. It is well known that the shear stress is proportional to the square of velocity while Eq. (15) implies linear proportionality between the shear stress and velocity.

For small β (sin $\beta \approx tan\,\beta = dD/dr$) Eq. (15) reduces to:

$$S_t = tan\,\beta = \frac{dD}{dr} = \frac{3\,\tau_o\ tan\,\delta_{vb}}{2\ g\ d\ (\rho_s - \rho)} \quad (16)$$

It is noted that in applying Eq. (16), the relation: tan δ_{vb} = 11 (*D*/*r*) has been used for the bed-shear deviation angle which means that the flow deviation angle is used in place of the bed shear stress deviation angle. The radial distribution for τ_o is taken by Bridge (1977) as:

$$\tau_o = \rho\ g\ D\ S_c\ \frac{r_c}{r} \quad (17)$$

Substituting Eq. (17) into Eq. (16), using the relation: tan δ_{vb} = 11 (*D*/*r*) and solving for the grain size (*d*), a relationship for grain-size distribution is obtained:

$$d = \frac{3\ \rho\ D\ S_c\ r_c}{2(\rho_s - \rho)\ r} \quad (18)$$

Odgaard (1986a), in a similar derivation such as by Ascanio and Kennedy (1983) with differences in using the critical condition based on grain roughness, presented the following equation for the transverse bed slope:

$$S_t = \tan\beta = \frac{3\,\alpha}{2}\ \frac{\sqrt{\tau_{*c}}}{\kappa}\ \frac{m+1}{m+2}\ F_d\ \frac{D}{r} \quad (19)$$

where, α is the projected area-volume ratio for a particle, normalized by that of a sphere (α = 1.27) and κ = 0.4.

Equation (19) is identical to an earlier version (Odgaard, 1984, his Eq. 5) which has been shown to be in agreement with laboratory and field data, Odgaard (1986a). Odgaard (1986a) used the fully developed equation for the transverse bed slope, Eq. (19), in his model equation for the stream-wise variation of the transverse bed slope. Bridge (1992) expressed that the assumption made by Odgaard (1986a) that the bed grains are at the threshold of motion (critical conditions for incipient motion) is unjustifiable. In addition, it was assumed that the lateral near-bed velocity is equal to the lateral water surface velocity (i.e., assuming a linear transverse velocity profile for fully developed flow). However, this is not necessarily true as could be seen in the velocity profile by Rozovskii (1957) for rough beds and Hafez (2024).

DOI: 10.3844/ajessp.2024.48.63

Odgaard (1982) assumed a straight transverse bed profile, the critical shear stress is proportional to $d^{-2/3}$, and obtained an equation for the distribution of the grain size as:

$$\frac{d}{d_c} = \left(\frac{D}{D_c}\right)^{5/3} \left(\frac{r_c}{r}\right)^{3/2} \quad (20)$$

where, d_c is the grain size at the channel center line. Regarding lateral bed-load movement, Ikeda (1982) studied lateral bed-load transport down the transverse bed slope in a straight channel and showed that:

$$\frac{q_*^r}{\tan\beta} = F\left(\frac{\tau_*}{\tau_{*c}}\right) \quad (21)$$

And:

$$q_*^r = \frac{q_b^r}{\sqrt{(s-1)g\,d^3}} \quad (22)$$

where, q_*^r is the dimensionless lateral bed-load transport per unit width, q_b^r is the lateral bed-load transport per unit width, τ_* is the dimensionless shear stress or the Shields stress, τ_{*c} is the critical Shields stress and s is the sediment particle specific gravity. Ikeda performed wind tunnel experiments using 0.26 and 0.42 mm sand and used other data from a water flume in order to determine the functional relationship in Eq. (21) and obtained:

$$\frac{q_*^r}{\tan\beta} = 0.0085\left[\frac{\tau_*}{\tau_{*c}}\left(\frac{\tau_*}{\tau_{*c}} - 1\right)\right]^{1/2} \quad (23)$$

Or:

$$q_b^r = 0.0085\tan\beta\,\sqrt{(s-1)g\,d^3}\left[\frac{\tau_*}{\tau_{*c}}\left(\frac{\tau_*}{\tau_{*c}} - 1\right)\right]^{1/2} \quad (24)$$

Parker (1984) argued that there are mechanistic differences between bed-load transport in air and water as τ_* is three or four times more in water than in air and that the functional relationship as given in Eq. (21) depends on the medium. Parker (1984) followed the concept that in curved alluvial channels, the prediction of lateral bed-load transport must include the effects of secondary currents in addition to the transverse bed slope. On the basis of the approach by Kikkawa *et al*. (1976); Parker (1984) presented the following formula for the lateral unit width bed-load discharge as follows:

$$\frac{q_b^r}{q_b^s} = \tan\delta_{vb} - \frac{1+(C_L/C_D)\tan\phi}{\tan\phi}\left(\frac{\tau_{*c}}{\tau_*}\right)^{1/2}\tan\beta \quad (25)$$

where, q_b^r and q_b^s are the lateral and longitudinal bed-load discharges per unit channel width, respectively, C_L and C_D are the lift and drag coefficients for sediment particles, respectively, ϕ is the sediment angle of repose and tan ϕ is the dynamic friction coefficient, $\tau*$ is the shields stress and τ_{*c} is the critical shields stress for incipient motion.

In the case of lateral equilibrium, q_b^r is zero, and Eq. (25) is reduced to:

$$S_t = \tan\beta = \frac{\tan\phi}{1+(C_L/C_D)\tan\phi}\left(\frac{\tau_*}{\tau_{*c}}\right)^{1/2}\tan\delta_{vb} \quad (26)$$

Equation (26) bears resemblance to transverse bed slope equations such as Eq. (7).

Hasegawa (1989) employed the following relation for the transverse bed-load transport rate:

$$q_b^r = q_b^s\left(\frac{v_{av}}{U} + \tan\delta_{vb} + T\,\frac{\partial\,\eta_b}{\partial\,r}\right) \quad (27)$$

where, v_{av} is the transverse component of the depth-averaged flow velocity, η_b is the downward displacement of the bed relative to a cross-sectional mean bed elevation and *T* is given by:

$$T = \sqrt{\frac{\tau_{*c}}{\mu_s\,\mu_k\,\tau_{*o}}} \quad (28)$$

where, μ_s and μ_k are the static and dynamic coefficients of Coulomb friction of the sediment particles, respectively and τ_{*o} denotes the cross-sectional average of τ_*. Equation (27) requires data that are difficult to obtain which precludes its use.

It is noted that in both of Eqs. (25 and 27) the lateral bed load transport rate depends on the longitudinal transport rate through tan (δ) which is called in the literature as tan (δ). Therefore, in these formulas, the well-known uncertainties in the longitudinal bed load rate is influencing the estimation of the lateral bed load rate. If a dam is built on a river that traps sediment in its upstream reservoir, then downstream of the dam the longitudinal bed-load transport will be small or almost vanishing. However, the author believes that the clear water downstream of the dam will have high stream power enough to erode the river banks producing sediment that could be transported laterally by the secondary currents or cross flow. Also, sediment might come from human activities on the banks that induce bank erosion or from tributary flow and this provides non-alluvial sediment to the river stream. Often downstream of dams as shown by Hafez (2022) river meandering increases to reduce the river's relatively high excess energy. The curvature of the river channel induces cross-flow associated with lateral bed-load transport which is almost independent of longitudinal bed-load transport. It is also assumed in Eq. (25) that the angle between the transverse and longitudinal bed-load discharges is the same as the flow velocity deviation angle in spite that the bed-load discharge is proportional to velocity to the third power. This is evident as the bed load rate is proportional to the bed shear stress to the power of 3/2 as in Meyer-Peter and Muller (1948) and the bed shear stress is proportional to the square of velocity).

The foregoing review asserts that in spite of the great efforts that existed in past works; still, there are still significant improvements that could be introduced as will be seen in the following section. In particular, answers are sought to the following questions. Could a differentiation

be made between the different deviation angles of the resultant: Flow velocity, boundary shear, and bed-load discharge? could an expression be developed for the thickness of the bed-load layer in curved channels which differs from that in straight channels? could the expression for the transverse bed slope be correctly and physically derived? could a transverse bed-load function be found that balances the inward transport due to secondary currents and the outward transport due to downslope movement by gravity? could an expression be developed for the longitudinal bed-load transport in curved and alluvial meandering channels? "can the developed equations be with a higher degree of physical realism"?

The following section will try to answer these important questions by developing innovative equations that improve the existing knowledge.

Materials and Methods

The Present Approach

First, recent equations developed by Hafez (2024) for the transverse flow velocity and the transverse boundary shear stress are used in this section; therefore, these equations are stated herein. Hafez (2024) expresses the transverse flow velocity, the transverse bed velocity, and the transverse bed or boundary shear stress, respectively as:

$$v = \frac{1}{\nu_T}\left(g\,S_r\left(\frac{z^2}{2} - D\,z\right) + \frac{\bar{U}^2\,(p+1)^2}{r\,(2p+1)}\left(D\,z - \frac{Z^{2p+2}}{D^{2p}\,(2p+2)}\right) \pm \frac{\tau_{rs}}{\rho}z\right) + v_b \quad (29)$$

where, ν_T is the turbulent viscosity, S_r is the transverse water surface slope, z is the vertical coordinate, $p = 1/m$ such that "m" is defined as in Eq. (5), τ_{rs} is the transverse shear at the water surface due to wind or ship forces or any lateral surface forces and v_b is the transverse bed velocity given by the following equation:

$$v_b = \frac{1}{\nu_T}\left(g\,S_r\left(\frac{D^2}{3}\right) - \frac{\bar{U}^2 D^2\,(p+1)\,(p+2)}{2\,r\,(2p+3)} \mp \frac{\tau_{rs}}{\rho}\frac{D}{2}\right) \quad (30)$$

For the boundary shear stress, the following equation is given which considers the transverse boundary shear stress a balancing the centripetal and the radial pressure forces unlike that in Ascanio and Kennedy (1983) who only considered balancing the centripetal force:

$$\tau_{or} = \rho\,D\,(\frac{\bar{U}^2\,(p+1)^2}{r\,(2p+1)} - g\,S_r) \quad (31)$$

Transverse Bed Slope

To determine an equation for the transverse bed slope, use is made of either: The model equation of Ascanio and Kennedy (1983), Eq. (1), or the model equation by Bridge (1977), Eq. (15), while in both cases adopting the relation developed for the lateral boundary shear stress by Hafez (2024), which is Eq. (31) herein.

Substitution is made of Eqs. (31 and 2) for the transverse boundary shear stress and the bed-load layer thickness, respectively with the inclusion of a correction factor, into the model equation of Ascanio and Kennedy (1983), Eq. (1), resulting in:

$$\rho\left(\frac{\bar{U}^2\,(p+1)^2}{r\,(2p+1)}\,D - g\,S_r\,D\right) = z_b(1-\lambda)(\rho_s - \rho)g\sin\beta \quad (32)$$

From Eq. (32), the following equation is obtained for the transverse bed slope in curved open channels assuming a small lateral bed slope angle, i.e., $S_t = \tan\beta \approx sin\,\beta$:

$$S_t = \sin\beta = \frac{\rho\,U_{*c}\,(\frac{\bar{U}^2\,(p+1)^2}{r\,(2p+1)}D - g\,S_r\,D)}{C_b\,d\,U_*\,(1-\lambda)(\rho_s-\rho)\,g} \quad (33)$$

It should be noted that Eq. (2) is used for z_b in Eq. (33) with the introduction of the correction factor, C_b, as proposed by Yeh and Kennedy (1993) which is later determined through calibration with data.

If the model equation by Bridge (1977), Eq. (15), is used, the following alternative equation is obtained for the transverse bed slope in curved open channels:

$$C_a\,\pi\left(\frac{d}{2}\right)^2\rho\,(\frac{\bar{U}^2\,(p+1)^2}{r\,(2p+1)}\,D - g\,S_r\,D) = \frac{4}{3}\,\pi\left(\frac{d}{2}\right)^3(\rho_s - \rho)\,g\sin\beta \quad (34)$$

where, C_a is a factor that accounts for sediment particles exposure to the acting lateral bed shear stress and it could be determined through calibration with data. Equation (34) after solving for the transverse bed slope becomes:

$$S_t = \sin\beta = \frac{3\,C_a\,\rho\,(\frac{\bar{U}^2\,(p+1)^2}{r\,(2p+1)}D - g\,S_r\,D)}{2\,(\rho_s-\rho)\,g\,d} \quad (35)$$

For small lateral bed slope angle, $S_t = tan\,\beta \approx sin\,\beta$ and from Eq. (12) $tan\,\beta = tan\,\delta_{vb}\,tan\,\phi$. Using these relations in Eq. (35), the following equation could be obtained for the lateral distribution of grain sizes:

$$d = \frac{3\,C_a\,\rho\,(\frac{\bar{U}(r)^2\,(p+1)^2}{r\,(2p+1)}D(r) - g\,S_r\,D(r))}{2\,(\rho_s-\rho)\,g\,(\tan\delta_{vb}\tan\phi)} \quad (36)$$

In Eq. (36) the local water depth and the depth-averaged velocity, depend in general on the radial distance through a functional dependence on r; this dependence could be given according to Ascanio and Kennedy (1983). Due to a lack of data, the transverse variation of the variables is not discussed herein and scope is limited to evaluating the variables at the central portion of the cross section.

Transverse Bed-Load Transport Rate

The lateral bed-load discharge per unit channel width could be assumed to be composed of two parts; the first is

the inward (toward the convex bank or the point bar side of the cross-section) transport due to the non-zero lateral bed velocity and the second is the outward transport (toward the concave bank) due to downslope movement by gravity on the transverse bed slope. Based on the lateral bed velocity equation that is developed by Hafez (2024), Eq. (30) herein, the following equation could be assumed for determining the lateral inward transport bed-load discharge per unit channel width as the product of the bed velocity and the thickness of the bed-load layer in curved channels as:

$$q_b^r = (s-1)(1-\lambda)\, z_b\, C_{vb} v_b \cos(\beta) \tag{37}$$

where, C_{vb} is a dimensionless coefficient that represents the portion of the lateral bed velocity that is transferred within the bed-load layer and to the moving bedload particles. It can be considered as an average velocity coefficient and cos (β) is used to get the component of the transverse bed load in the direction of the transverse bed slope. The right-hand side of Eq. (37) represents the bed-load transport by secondary currents up the transverse bed slope.

Using Eq. (24) by Ikeda (1982) for the downslope movement by the gravity of the bed particles and Eq. (2) for z_b with the correction factor C_b in addition to Eq. (37), the following equation is obtained for the lateral bed-load transport rate:

$$q_b^r = (s-1)(1-\lambda)\, C_b\, d\, \frac{U_*}{U_{*c}}\, C_{vb} v_b \cos(\beta) - 0.0085 \tan\beta \sqrt{(s-1) g\, d^3} \left[\frac{\tau_*}{\tau_{*c}}\left(\frac{\tau_*}{\tau_{*c}} - 1\right)\right]^{1/2} \tag{38}$$

It should be noted that the correction factor C_b is introduced in Eq. (38) to reflect the thickness of the bed-load layer in curved channels as being different from that in straight channels. Substituting Eq. (29) for the lateral bed velocity in Eq. (38) results in:

$$q_b^r = \left\{(s-1)(1-\lambda)\frac{C_b}{U_{*c}^2}\frac{C_{vb}}{\nu_T}\left[g S_r\left(\frac{D^2}{3}\right) - \frac{\bar{U}^2 D^2 (p+1)(p+2)}{2r(2p+3)} \mp \frac{\tau_{rs}}{\rho}\frac{D}{2}\right]^2\right\}\cos(\beta) - \{0.0085 \tan\beta \sqrt{(s-1) g\, d^3} \left[\frac{\tau_*}{\tau_{*c}}\left(\frac{\tau_*}{\tau_{*c}} - 1\right)\right]^{1/2} \tag{39}$$

Equations (38 or 39) are called the Modified-Ikeda lateral bed-load transport equation.

The second part on the right-hand side of Parker (1984), Eq. (25), expresses the lateral bed load transport downslope of the transverse bed. It could be adopted in the present approach to express the downslope component of the lateral bed-load discharge. By subtracting this downslope component in Parker (1984) equation from the lateral upslope transport, Eq. (37), while substituting Eq. (2) for z_b with the correction factor C_b, the following equation for the lateral bedload rate results in:

$$q_b^r = (s-1)(1-\lambda) C_b\, d\, \frac{U_*}{U_{*c}} C_{vb} v_b \cos(\beta) - \frac{[1+(C_L/C_D)\tan\phi]}{\tan\phi}\left(\frac{\tau_{*c}}{\tau_*}\right)^{1/2} \tan\beta\, \frac{q_b^r}{\tan\delta_{q_b}} \tag{40}$$

where, in Eq. (40) the relation: $q_b^s = \frac{q_b^r}{\tan\delta_{q_b}}$ is substituted for the longitudinal unit bed-load discharge (q_b^s) in area units (m^2/s). The bed load deviation angle ($\tan\delta_{q_b}$) could be given by Eq. (49) given thereafter.

Now solving in Eq. (40) for the lateral bed load rate yields:

$$q_b^r = \frac{(s-1)(1-\lambda) C_b\, d\, \frac{U_*}{U_{*c}} C_{vb} v_b \cos(\beta)}{\left\{1 + \frac{[1+(C_L/C_D)\tan\phi]}{\tan\phi}\left(\frac{\tau_{*c}}{\tau_*}\right)^{1/2}\frac{\tan\beta}{\tan\delta_{q_b}}\right\}} \tag{41}$$

It is noted that Eq. (41) has an advantage over the equation of Parker (1984), Eq. (25), in that it does not include the highly uncertain longitudinal bed load rate (q_b^s). Eq. (41) is called the modified-parker equation.

Flow Velocity, Boundary Shear Stress, and Bed-Load Rate Deviation Angles

In this study distinction is made between the near bed resultant flow velocity deviation angle, the resultant bed shear stress deviation angle, and the resultant bed-load discharge deviation angle as in the following. The primary-flow velocity power law given by Zimmerman and Kennedy (1978) is:

$$\frac{u}{\bar{U}} = \frac{m+1}{m}\, \eta^{1/m} = (1+p)\, \eta^{1/m} \tag{42}$$

where, p =1/m. The power law was used in many meandering investigations such as Ascanio and Kennedy (1983); Chang (1983-1984); Odgaard (1986a). Recently in a different, with some similarities, (Dey *et al*., 2023) adopted the power law for the stream-wise velocity in their investigation of flow over a downstream-skewed wavy bed in which flow curvature is in the vertical plane, Hafez (2024).

The longitudinal surface velocity could be obtained from Eq. (42) by letting $z = D$ to get:

$$u_s = \bar{U}(1+p) \tag{43}$$

The surface velocity deviation angle, δ_{vs}, could be given according to Eq. (29), Hafez (2024), by substituting $z = D$ and Eq. (43) as:

$$\tan\delta_{vs} = \frac{v_s}{u_s} = \frac{1}{\bar{U}(p+1)\nu_T}\left(-\frac{D^2}{2} g S_r + \frac{\bar{U}^2 D^2 (p+1)}{2r} \pm \frac{\tau_{rs}}{\rho} D\right) + \frac{v_b}{\bar{U}(p+1)} \tag{44}$$

The flow bed velocity deviation angle, δ_{vb}, using Eq. (30) for v_b, could be given, by 3Hafez (2024) as:

$$\tan\delta_{vb} = \frac{v_b}{u_b} = \frac{1}{u_b \nu_T}\left(\frac{g S_r\left(\frac{D^2}{3}\right) - }{\frac{\bar{U}^2 D^2 (p+1)(p+2)}{2r(2p+3)} \mp \frac{\tau_{rs}}{\rho}\frac{D}{2}}\right) \tag{45}$$

There are several ways to determine u_b in Eq. (45) such as from the vertical distribution of the longitudinal main velocity or from a bed-load formula and the thickness of the bed-load layer. Hafez (2024) based on the well-known logarithmic velocity distribution over the rough boundary, assumed $u_b \approx 8.5\, u_*$ and u_* is the local shear velocity. However; the determination of the near-bed velocity is not an easy task.

The resultant bed shear stress deviation angle, $\delta_{\tau b}$, Hafez (2024), using Eq. (31) for τ_{or}, could be given as:

$$tan\,\delta_{\tau b} = \frac{\tau_{or}}{\tau_o} = \frac{\rho\left(\frac{\overline{U}^2\,(p+1)^2}{r\,(2p+1)}\,D - \,g\,S_r\,D\right)}{\rho\,\frac{\overline{U}^2\,f}{8}} = \frac{8\,(\frac{\overline{U}^2\,(p+1)^2}{r\,(2p+1)}D - g\,S_r\,D)}{\overline{U}^2\,f} \quad (46)$$

The bed-load resultant discharge deviation angle, δ_{q_b}, using Eq. (41) for q_b^r, could be given as:

$$\tan\delta_{q_b} = \frac{q_b^r}{q_b^s} = \frac{\frac{(s-1)\,(1-\lambda)\,C_b\,d\,\frac{U_*}{U_{*c}}\,c_{vb}v_b\cos(\beta)}{\left\{1+\frac{[1+(C_L/C_D)\,\tan\phi]}{\tan\phi}\left(\frac{\tau_{*c}}{\tau_*}\right)^{1/2}\frac{\tan\beta}{\tan\delta_{q_b}}\right\}}}{q_b^s} \quad (47)$$

where, q_b^s could be given using a suitable longitudinal bed load formula (such as for example the longitudinal bed load by Meyer-Peter and Muller (1948) and v_b could be given by Eq. (30). However, Eq. (47) suffers from its dependency on the longitudinal bed-load discharge (q_b^s) which is difficult to be determined. Most bed load equations use the critical Shields stress criterion while (Perret *et al*., 2023) data show a large scatter in the critical Shields stress values for initial. A different and more convenient way could be used for determining the deviation angle of the resultant flow velocity and the resultant bed-load discharge based on the deviation angle of the resultant boundary shear stress. It is hypothesized herein that the equation of the deviation angle for the resultant bed shear stress has considerable confidence due to knowledge with reasonable accuracy of the lateral and longitudinal boundary shear stresses. For the other two equations, Eqs. (45 and 47), the requirement of accurately knowing the longitudinal bed velocity and longitudinal bed load puts considerable uncertainties in using these equations. Most of the developed bed load equations represent instantaneous bedload transport related to temporal hydraulic and bed conditions and are not well-suited to estimate long-term average bedload over a broad range of channels, Braithwaite (2023).

It is commonly assumed that the shear stress is proportional to the square of the flow velocity while the bed-load transport is proportional to the shear stress to the power of 1.5 according to Meyer-Peter and Muller (1948), Eq. (59) thereafter. The same proportionality would be assumed to be applicable to the deviation angles. For example, it can be stated that: $tan\,\delta_{\tau b} = \frac{\tau_{or}}{\tau_o} \sim \frac{\rho\,{v_b}^2}{\rho\,{u_b}^2} = \frac{{v_b}^2}{{u_b}^2} = (tan\,\delta_{vb})^2$. Applying the last relation while substituting the deviation angle for the bed shear stress from Eq. (46) yields:

$$tan\,\delta_{vb} = \sqrt{tan\,\delta_{\tau b}} = \sqrt{\frac{8\,(\frac{\overline{U}^2\,(p+1)^2}{r\,(2p+1)}D - g\,S_r\,D)}{\overline{U}^2\,f}} \quad (48)$$

Using the same methodology to the bed load deviation angle results in:

$$\tan\delta_{q_b} = (\tan\delta_{\tau b})^{1.5} = (\frac{8\,(\frac{\overline{U}^2\,(p+1)^2}{r\,(2p+1)}D - g\,S_r\,D)}{\overline{U}^2\,f})^{1.5} \quad (49)$$

where, $(tan\,\delta_{\tau b})$ is given as by Eq. (46). Comparing Eqs. (49 and 47), it can be seen that Eq. (49) has the advantage of including the main velocity and roughness effects in addition to the inclusion of the water depth and radius of curvature while Eq. (47) includes the highly hard to obtain with accuracy the longitudinal bed load discharge. In addition, Eq. (49) has a simpler structure than Eq. (47).

The foregoing developed equations for the lateral bed velocity and the flow bed-velocity deviation angle allow for determining the longitudinal bed-load discharge in an alluvial meandering or curved river reach which has not been done to the best of the knowledge of the writer. From Eq. (45) the longitudinal bed velocity in curved reach could be given as $u_b = v_b\,cot\,\delta_{vb}$, where v_b could be obtained from Eq. (30) and $cot\,\delta_{vb}$ could be obtained as the reciprocal of the left-hand side of Eq. (48). The longitudinal unit bed-load discharge only due to curvature, $(q_b^s)_{crv}$, could be then given as:

$$(q_b^s)_{crv} = C_{qb}\,u_b\,z_b = C_{qb}\,v_b\,cot\,\delta_{vb}\,z_b \quad (50)$$

where, C_{qb} is a coefficient that relates the average velocity within the bed-load layer to the bed-load velocity at the top edge of the bed layer (could be taken as 0.5), u_b is given according to Eq. (50) and z_b is given according to Karim (1981) formula, Eq. (2) corrected using C_b. It is important to stress that Eq. (51) is valid only for curved or meandering reaches and it requires the existence of a transverse bed velocity. Now, the total longitudinal bedload transport rate $(q_b^s)_{tot}$ could be given as:

$$(q_b^s)_{tot} = (q_b^s)_{str} + (q_b^s)_{crv} \quad (51)$$

where, $(q_b^s)_{str}$ is the longitudinal bed load transport due to the longitudinal energy slope while $(q_b^s)_{crv}$ is the longitudinal bed load transport due to curvature of the river channel resulting from non-zero net transverse bed load rate and is given by Eq. (50). Although most river reaches are rare to be straight over 10-12 channel widths, Odgaard (1986a), most sediment morphological models such as the well-known and widely used HEC-RAS, Brunner (2016), considers only the straight longitudinal bed load rate. Equation (51) is valid for any river that

DOI: 10.3844/ajessp.2024.48.63

reaches straight or curved. If the reach is straight ($r \to \infty$ and v_b would be zero) then $(q_b^s)_{crv}$ would be zero.

Results and Discussion

Application of the Theoretical Formulations to Two Sets of Field Data

Valuable field data exist for the Fall River, Rocky Mountain National Park, by Thorne *et al*. (1983) and for Muddy Creek, Wyoming, by Dietrich and Smith (1983). "These reaches were selected for verification because they cover a complete or near complete cycle of secondary-flow development and decay through two-consecutive meander bends. Because of their small radius of curvature, the bends offer a significant challenge to the theory. Both bends show a substantial variation in bed topography over a very short distance." Odgaard (1986b). The author agrees with Odgaard (1986b) in that these two cases are characterized by strong meandering structure making each case a well-known case study and a significant challenge to the equations developed from the bend theory.

For a reach of 110 m in the Fall River, the values of the mean water depth, width, depth-averaged velocity, discharge, longitudinal water surface slope, and median grain diameter are 0.34, 7.8 m, 0.49 m/s, 1.4 m^3/s, 0.00173 and 0.2 mm, respectively. The calculated Manning roughness coefficient in metric units (s/[$m^{1/3}$]) from the Manning equation is 0.0414 s/[$m^{1/3}$] (f = 0.192) and the Shields factor is 0.035. In all runs the von Karman constant is taken as 0.4 and the bed porosity as 0.4, Odgaard (1986b).

Table 1 shows calculations of the transverse bed slope in the Fall River using different equations in the first reach at Section 1, which is shown in Fig. (1). At Section 1 the radius of curvature is equal to 52 m for which the measured transverse bed slope is about 0.0388 according to data by Thorne *et al*. (1983). Section 2 is located near the exit of the first bend where fully developed flow conditions often exist near the bends' exit. In spite of that Eqs. (6-7) predict a very close value, with Eq. (7) prediction being better, it should be kept in mind that the bed-layer thickness equation, Eq. (2), which is based on straight channel condition was used for the bed-load layer thickness for this case of a curved river reach. Indeed, this bed-layer thickness should be considerably smaller than the thickness due to straight conditions, because the bed-shear and bed-load transport in straight channels are considerably higher and more intense than their equivalents in curved reaches. Using the large straight thickness of the bed load layer which is supposed to be in the denominator of the equation would yield a small transverse bed slope. To compensate for that, an increase in the lateral bed shear by Ascanio and Kennedy (1983) must occur by dropping the transverse water surface slope contribution from Eq. (4) because of its negative sign. Equation (6) uses the original equation for the lateral bed shear while Eq. (4) is without the use of the simplified Nunner's relation. Although in both cases the results are very close, nonetheless, conceptually speaking these two Eqs. (6-7) suffer from the aforementioned assumptions of using the longitudinal bed-layer thickness and a boundary shear formula which does not include the transverse pressure force.

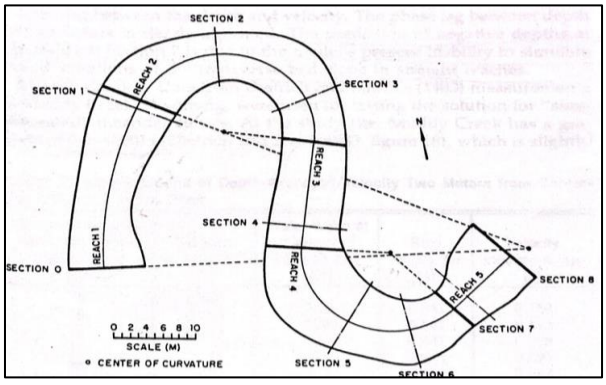

Fig. 1: Discretization of Fall River, after Odgaard (1986b)

Table 1: Prediction of the transverse bed slope (S_t) at the Fall River and Muddy Creek, USA

	Manning's roughness, n	S_t measured	S_t Eq. (6)	S_t Eq. (7)	S_t Eq. (16)	S_t Eq. (19)	S_t Eq. (26)*	S_t Eq. (33)$	S_t Eq. (35)&
Fall River, Calibration, section 1, r_c = 52 m	0.0414	0.0388 at section 1	0.034	0.038	0.192	0.039	0.205 0.190 0.171 0.041	0.038 0.021 0.013 0.010	0.031 0.040 0.046 0.062
Fall River, verification, r_c = 11 m	0.0414	0.185 at section 2,	0.162	0.180	0.909	0.185	0.194	0.181	0.189
Muddy Creek, verification, r_c = 8 m	0.0369	0.167 at section 22	0.172	0.191	0.400	0.197	0.153	0.173	(0.088, C_a =0.65) (0.136, Ca = 1.0)

*Calibration values of C_L/C_D = 0.008, 0.2, 0.5 and 10.0, respectively
$Calibration values of C_b = 0.25, 0.45, 0.75 and 1.0, respectively
&Calibration values of C_a = 0.5, 0.65, 0.75 and 1.0, respectively
Values in red represent the best match of predictions with the measured data

Equation (16) by Bridge (1977) highly over-predicts the transverse bed slope by about 5 times which is due to the used form for the lateral bed shear as τ_o tan (δ_{vb}) in addition to assuming the whole magnitude of this bed shear to be transferred to the bed-particles without considering any sheltering or shear-reduction effect. Equation (19) by Odgaard (1986a) provides an excellent match, however, as stated before a fundamental weakness lies in its assumption of the incipient motion of the bed particles as pointed out by Bridge (1992). Another assumption of Eq. (19) is the equality of the lateral bed and surface velocities but this approximation can be accepted as the two velocity values although are not often equal, however, they could be close.

Equations (26), (33), and (35) have unknown coefficients that are determined through calibration. As shown in Table (1) for Eq. (26) a ratio of the lift to drag coefficient of 10 produced the best prediction. Bridge (1992) reports a ratio of 0.008 at the threshold of motion while it approaches infinity at the threshold of suspension. If the ratio C_L/C_D of 10.0 seems to be unrealistic it can be assumed that in Eq. (26) the ratio C_L/C_D is replaced by a factor Co*(C_L/C_D) which is assumed equal to 10.0 with Co is a calibration coefficient equal to 10 divided by the actual lift/drag ratio.

Equation (33) gives best results when C_b is 0.25. This value will be confirmed when field data for the muddy creek and the Fall River are used later for calibration and verification of this coefficient as seen in Table 1. It means that the thickness of the bed-load layer in curved channels at these flow and sediment conditions is one-quarter of the thickness of the bed-load layer in straight channels.

Ascanio and Kennedy (1983) used a longitudinal bed-shear-stress reduction factor where a value of 0.43 was considered by them for a friction factor of 0.165. Similarly, a reduction factor C_a could be justified when it is used for the lateral bed shear stress. This factor should be dependent on the bed-particle size and so should the factor C_b. A value for C_a of 0.65 was found to have a transverse bed slope of 0.04 versus a measured value of 0.0388 as seen in Table (1) where the friction factor is 0.193. Since complete field data are hard to find in which all the required hydraulic, sediment, and topographical data exist, a trial will be made herein for calibration and verification of the aforementioned constants.

Table 1 shows the prediction of the transverse bed slope at the Fall River in section 2, Fig. (1), where the radius of curvature is 11 m and the measured transverse bed slope is 0.185. Equations (19), (33), and (35) provide very close values followed by Eqs. (7) and (26) while Eq. (16) predicts about 5 times the measured value. It is seen that Eqs. (26), (33), and (35) using the calibrated coefficients predict very well the transverse bed slope which indicates success in the calibration process.

For a reach of 40 m in the Muddy Creek, the values of the mean water depth, width, depth-averaged velocity, discharge, longitudinal water surface slope, and median grain diameter are 0.40, 4.0 m, 0.55 m/s, 1.1 m^3/s, 0.0014 and 0.7 mm, respectively, Odgaard (1986b). The calculated manning roughness coefficient is 0.0369 (f = 0.145) and the shields factor is 0.04. The lateral water surface slopes based on measured water surface elevations are 0.003 at section 19 A and 0.004 at section 18 which are located at the bend apex. The calculated transverse water surface slope (S_r) from Eq. (52) with the coefficient C_r = 1, Rozoveskii (1957), is 0.00385, and using Eq. (53), Hafez (2023) when dividing Δz by the width B to yield the lateral water surface slope (S_r) yields 0.00412 compared to a measured value of 0.004. These predictions support the bend theory equation for predicting the lateral water surface slope and the use of Eqs. (52) or (53) when values of the transverse water surface slope are required. Equation (53) has an advantage over Eq. (52) in that it includes channel roughness effects via the parameter p:

$$S_r = \frac{C_r \bar{U}^2}{g\, r_c} \tag{52}$$

$$\Delta z = \frac{(1+p)^2}{(2p+1)} \frac{\bar{U}^2 B}{g\, r_c} or\ S_r = \frac{(1+p)^2}{(2p+1)} \frac{\bar{U}^2}{g\, r_c} \tag{53}$$

where, Δz is the difference in height between the outer and the inner banks and r_c is the channel centreline radius of curvature.

Table 1 shows for muddy creek the prediction by Eqs. (6) and (33) give excellent match to the measured data. Equation (16) predicts a very high value, while Eqs. (7), (26), and (35) predict close values. The prediction by Eq. (35) deserves some explanation. For a C_a value of 0.65, the predicted slope is almost half the measured value but when C_a = 1 the prediction improves to be 81% of the measured slope. It should be remembered that the calibrated value of 0.65 was based on a grain diameter of 0.2 mm at Fall River while the grain diameter used in Muddy Creek is 0.7 mm which is more than 3 times larger. It is expected that larger particles have less sheltering effect than smaller ones and a value of C_a = 1 could be assumed in this case which produces a lateral bed-slope of 0.136 (81% of the measured value). The 0.7 mm grain diameter was reported by Odgaard (1986b) to be the median grain size while Dietrich and Smith (1984) reported measured grain diameters in Muddy Creek which vary from 0.3-2.0 mm depending upon the location in the stream. Indeed this discussion points out the importance of the accuracy of the measured data especially grain sizes as Eq. (35) is very sensitive to grain sizes.

Now, after this detailed analysis of the existing and developed equations herein for predicting the fully developed transverse bed-slope (S_t) is made, these equations could be used in investigating the stream-wise

variation of S_t as was done in Odgaard (1986b) which presented the following Eq. (34) in Odgaard (1986a):

$$S_{Tc} = S_{Tco} - (S_{Tco} - S_{Tci})\, E \tag{54}$$

where, S_{Tc} is the transverse bed-slope at a stream-wise distance (x) along the channel center line, S_{Tco} is the fully developed transverse bed-slope which could be given using the equations developed herein (i.e., $S\_Tco = S_t$), S_{Tci} is the initial transverse bed-slope (at x = 0; x = distance along channel axis) and E is a function which depends on the relative distance (x/B) where B is the channel width. This equation points to the need for fully developed or uniform quantities when analyzing non-uniform conditions.

Table 2 shows stream-wise computations of the transverse bed slopes in the Fall River using Eq. (54). The discretization of the Fall River according to Odgaard (1986b) is that reach 1 is between sections 0-1, reach 2 is nearly between sections 1-3, reach 3 is nearly between sections 3 and 4, reach 4 is nearly between sections 4 and 7 and reach 5 is between sections 7-8. Two approaches are used in Table 2, the first is by Odgaard (1986b) in which the fully developed transverse bed-slope Eq. (19) is used, while the second uses Eq. (33) by the present approach with C_b = 0.25. The same values of the function, E, are used in the present approach as it is only a distance function. Table (2) shows very good agreement between the two approaches.

It can be concluded that Eq. (33) with the proper value for C_b resembles Eqs. (6-7) by Ascanio and Kennedy (1983), but with the correct form for the transverse boundary shear stress and the thickness of the transverse bed-load layer. This makes Eq. (33) more conceptually and physically correct than Eqs. (6-7), in spite that the predicted numeric values are nearly equal.

The data of the measured transverse bed slope by Zimmerman and Kennedy (1978) fit linearly Eq. (7) by Ascanio and Kennedy (1983) with a slope equal to 1.3. This means that $\frac{(8\,\tau_{*c})^{1/2}}{(1-\lambda)}$ in Eq. (7) is 1.3 according to 50 data points. These data could be used to calibrate the correction factor for the thickness of the bed-load layer in curved channels assuming that the straight line with slope 1.3 fits the measured data well. Equation (33) could be cast in the following form:

$$S_t = \left[\frac{p^2\,(1+2\,f^{1/2})}{C_b\,(2p+1)(1+f^{1/2})f^{1/2}}\right] \frac{D}{r}\, F_d\, \frac{(8\,\tau_{*c})^{1/2}}{(1-\lambda)}\, \frac{1+f^{1/2}}{1+2\,f^{1/2}} \tag{55}$$

For Eq. (55) to be representing the experimental data of the transverse bed slope by Zimmerman and Kennedy (1978), the quantity in the square bracket on the right-hand side should be unity. This causes Eq. (55) to be exactly equivalent to Eq. (7) by Ascanio and Kennedy (1983). The use of the lateral distribution of velocity and slope as by Ascanio and Kennedy (1983) yields exactly Eq. (11) which fits very well through the experimental data of Zimmerman and Kennedy (1978), the transverse bed profiles from experiments by Zimmermann (1974) and the Missouri River data by Falcon-Ascanio (1979). However, the present approach has a higher degree of physical realism than that by Ascanio and Kennedy (1983) because it considers more realistic lateral boundary shear stress and thickness of the bed load layer in meandering channels. The employed bed shear stress formulation is more realistic because it expresses that the transverse boundary shear stress balances the centripetal and the radial pressure forces unlike that by Ascanio and Kennedy (1983) who only considered balancing the centripetal force.

Table 2: Computations of transverse bed slopes along the center line in Fall River

Reach number	r_c (m)	S_{Tci}, Odgaard (1986b)	S_{Tco}, Odgaard (1986b)	Section number	Distance from beginning of reach (m)	Value of function, E	S_{Tci}, present approach	S_{Tco}, present approach, Eq. (33)	S_{Tc}, using Eq. (33) for S_{Tco}	S_{Tc}, Odgaard (1986b)
1	52	0	0.039	1	23	-0.42	0.000	0.038	0.054	0.055
					24	-0.45	0.000	0.038	0.055	0.057
2	11	0.057	0.185	2	12	0.28	0.055	0.181	0.146	0.149
				3	25	-0.46	0.055	0.181	0.239	0.244
				End	32	-0.39	0.055	0.181	0.230	0.235
3	∞	0.235	0	4	12	0.28	0.230	0.000	0.064	0.066
				End	15	0.03	0.230	0.000	0.007	0.007
4	11	0.007	0.185	5	12	0.28	0.007	0.181	0.132	0.135
				6	20	-0.30	0.007	0.181	0.233	0.238
				End	23	-0.42	0.007	0.181	0.254	0.260
5	∞	0.26	0	7	5	0.84	0.254	0.000	0.213	NA
				8	13	0.19	0.254	0.000	0.048	0.049

DOI: 10.3844/ajessp.2024.48.63

From this condition of unity the following equation for C_b results:

$$C_b = \frac{p^2\,(1+2\,f^{1/2})}{(2p+1)(1+\,f^{1/2})f^{1/2}} \tag{56}$$

This equation expresses the correction factor C_b in terms of the friction factor and von Karman constant which means its dependency on the grain sizes (a measure of bed load) and suspended load. Replacing the friction factor by its equivalency in terms of Manning's roughness coefficient, results in the graph shown in Fig. (2). It is interesting to note that Manning's roughness coefficient equals about 0.04 (which is very close to the roughness values at Fall River and Muddy Creek) the value of C_b is 0.25 which supports the previous calibration process. Equation (56) for C_b suggests that the bed-load layer thickness in curved channels (z_{br}) could be given as:

$$z_{br} = C_b\; d\; \frac{U_*}{U_{*c}} = \frac{p^2\,(1+2\,f^{1/2})}{(2p+1)(1+\,f^{1/2})f^{1/2}}\; d\; \frac{U_*}{U_{*c}} \tag{57}$$

Now, the hydraulic and sediment data of Muddy Creek are used for the calculation of the lateral bed-load rate under varying roughness conditions. Manning's roughness coefficient (n) is changed in increments with corresponding variations in the energy slope (S) according to manning's formula:

$$S = \frac{n^2\,Q^2}{B^2\,{R_H}^{10/3}} \tag{58}$$

where, Q is the water discharge, B is the channel width and R_H is the hydraulic radius. In applying Eq. (25) by Parker (1984) the longitudinal bed load rate is required. In this context, the Meyer-Peter and Muller (1948) bed load formula is used which is given as:

$$\left[\frac{q_b\,(\gamma_s-\gamma)}{\gamma}\right]^{2/3} \rho^{1/3}\;\frac{0.25}{(\gamma_s-\gamma)D_s} = \frac{(k_s/k_r)\,\gamma\,R_H\,S}{(\gamma_s-\gamma)D_s} - 0.047 \tag{59}$$

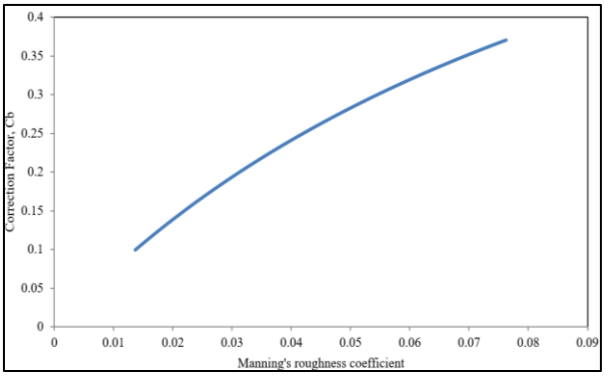

Fig. 2: Variation of the correction factor, *Cb*, for the lateral bed-layer thickness versus Manning's roughness coefficient

where, q_b is the bed-load discharge in weight per unit time and unit channel width, γ_s is the sediment unit weight, γ is the water unit weight, k_s is a roughness coefficient according to Strickler based on the energy gradient caused by skin friction and K_r is a roughness coefficient according to the total energy gradient. In the absence of bedforms, (k_s/k_r) could be assumed unity according to Chang (1992). The unit bed load rate (q_b) which is weight-based is divided by γ_s to get q_b^s in units of area/time. To apply Eq. (25), tan (δ_{vb}) is taken as $11(D/r_c)$ according to Rozovskii (1957).

The bed velocity coefficient appearing in Eqs. (38 and 41) is assumed as 0.1 as follows. If the bed-load layer were filled completely with water and the bed velocity is v_b at the top of the bed-load layer and zero at the bottom immobile bed, then the average bed velocity would be 0.5 v_b assuming linear variation. Since the bed-load layer is filled mostly with sediment particles which are heavier than the water molecules the average velocity within the bed-load layer would be less than 0.5 v_b as much friction exists between the sediment particles than between the water molecules. Therefore, a value of 0.1 v_b seems a reasonable assumption and its exact value should be considered in future research. To apply Eqs. (25 and 39), the required transverse bed-slope, tan (β), is selected as that by Eq. (33) where C_b is given according to Eq. (56). Since this bed-load transport rate is under fully developed conditions, the transverse bed-load discharge should be zero or at least becomes close to zero.

The calculations of the lateral bed-load transport using different equations are shown in Tables (3-4), Figs. (3-4). It is seen in Table (3) and Fig. (3), that Ikeda's equation values for the downslope transport, Eq. (24), are very small so all the transverse bed-load is due to the upslope transport as by Eq. (37). This deficiency makes Eq. (39) not a suitable equation for calculation of the transverse bed-load rate which is in line of Parker (1984) reservation on Ikeda's equation. It is apparent from Fig. (4), Eq. (25) by Parker (1984) produces highly transverse bed-load rates which are much larger than those by the present approach by Eq. (41). Equation (41) where the upslope inward transport is due to the present approach, Eq. (37), while the downslope transport is due to Parker (1984) seems to produce very small lateral bed load transport rates as seen in Fig. (4). It should be noted that the hydraulic data for the Muddy creek cannot be guaranteed to represent fully developed conditions, i.e., it might represent quasi fully developed conditions and therefore a perfect zero lateral bed load rate should not be expected. It is seen from Table (3) that the downslope component of the lateral bed-load rate is higher by two orders of magnitudes by Parker (1984) equation than by Ikeda (1982) equation. Comparing the corresponding values in Tables (3-4) where the quantity C_L/C_D is 10.0 in the former and 1.0 and 0.5 in the latter, shows that its effect

is not significant although the variation of C_L/C_D is of an order of magnitude. Schmeeckle *et al*. (2007) made direct measurements of lift and drag over a gravel bed, but also in low gradient streams with deep flow. They found for spherical particles that $C_D \approx 0.76$ and that C_L was highly variable. For fully submerged particles (Lamb *et al*., 2017) in their Direct measurements of lift and drag on shallowly submerged cobbles in steep streams found that drag coefficients for spheres increase systematically from $C_D \approx 0.1$-$C_D \approx 0.7$ while the lift coefficients for fully submerged particles vary from $0.06< C_L <4$. Thus, the values selected herein for the quantity C_L/C_D are within the experimental findings while a precise determination is recommended in future research.

Table 3: Calculations of transverse bed-load transport discharge (cm^2/s) using data from Muddy Creek

Manning's roughness, n	Only upslope transport Eq. (37), (cm^2/s)	Ikeda (1982), only downslope transport Eq. (24), (cm^2/s)	Modified-Ikeda, Eq. (39), (cm^2/s)	Only downslope transport, from Eq. (25), (cm^2/s)	Parker* (1984), Eq. (25), (cm^2/s)	Modified-Parker*, Eq. (41), (cm^2/s)
0.013	0.118	0.0002	0.117	0.008	0.014	0.038
0.019	0.166	0.0007	0.165	0.044	0.087	0.052
0.023	0.203	0.0013	0.201	0.092	0.198	0.062
0.027	0.234	0.0019	0.232	0.147	0.339	0.071
0.030	0.261	0.0026	0.258	0.208	0.506	0.078
0.033	0.286	0.0034	0.282	0.273	0.696	0.084
0.035	0.308	0.0042	0.304	0.342	0.907	0.090
0.038	0.329	0.0050	0.324	0.413	1.138	0.095
0.040	0.349	0.0058	0.342	0.487	1.388	0.100
0.042	0.367	0.0066	0.360	0.563	1.656	0.104
0.044	0.385	0.0075	0.377	0.641	1.940	0.108
0.046	0.402	0.0084	0.393	0.721	2.240	0.112
0.048	0.418	0.0093	0.408	0.803	2.556	0.116
0.050	0.433	0.0103	0.422	0.886	2.886	0.120
0.051	0.448	0.0112	0.436	0.970	3.231	0.123
0.053	0.462	0.0122	0.449	1.056	3.590	0.126
0.055	0.476	0.0131	0.462	1.142	3.962	0.129
0.056	0.490	0.0141	0.475	1.230	4.347	0.132
0.058	0.503	0.0151	0.487	1.319	4.745	0.135
0.059	0.516	0.0161	0.499	1.409	5.156	0.138
0.061	0.528	0.0171	0.510	1.499	5.579	0.140

*C_L/C_D =10.0

Table 4: Calculations of transverse bed-load transport discharge (cm^2/s) using data from Muddy Creek

Manning's roughness, n	Only downslope transport, from Eq. (25), (cm^2/s)	Parker (1984), Eq. (25), at C_L/C_D =1.0 (cm^2/s)	Parker (1984), Eq. (25), at C_L/C_D = 0.5 (cm^2/s)	Only downslope transport, from Eq. (25), (cm^2/s)	Modified-Parker, Eq. (41), at C_L/C_D =1.0 (cm^2/s)	Modified-Parker, Eq. (41), at C_L/C_D = 0.5 (cm^2/s)
0.013	0.002	0.019	0.020	0.002	0.077	0.082
0.019	0.011	0.120	0.121	0.009	0.107	0.114
0.023	0.023	0.267	0.270	0.019	0.130	0.138
0.027	0.037	0.449	0.455	0.031	0.148	0.158
0.03	0.052	0.662	0.670	0.043	0.164	0.175
0.033	0.068	0.901	0.912	0.057	0.179	0.190
0.035	0.085	1.163	1.178	0.071	0.192	0.204
0.038	0.103	1.448	1.465	0.086	0.204	0.217
0.04	0.122	1.753	1.774	0.101	0.215	0.229
0.042	0.141	2.078	2.101	0.117	0.225	0.241
0.044	0.160	2.421	2.447	0.134	0.235	0.251
0.046	0.180	2.781	2.811	0.150	0.244	0.261
0.048	0.201	3.158	3.191	0.167	0.253	0.271
0.05	0.221	3.550	3.587	0.185	0.261	0.280
0.051	0.243	3.958	3.999	0.202	0.269	0.289
0.053	0.264	4.381	4.425	0.220	0.277	0.297
0.055	0.286	4.819	4.866	0.238	0.285	0.305
0.056	0.308	5.270	5.321	0.256	0.292	0.313
0.058	0.330	5.735	5.790	0.275	0.299	0.321
0.059	0.352	6.213	6.271	0.294	0.306	0.328
0.061	0.375	6.703	6.766	0.312	0.312	0.335

DOI: 10.3844/ajessp.2024.48.63

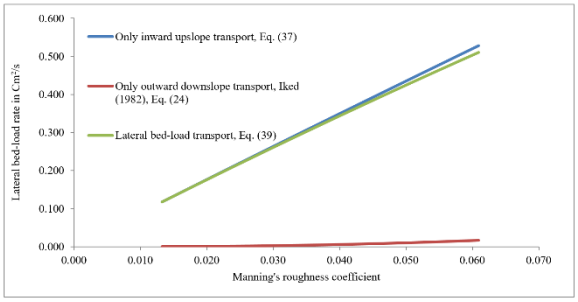

Fig. 3: Components of the lateral bed-load transport by modified-Ikeda equation

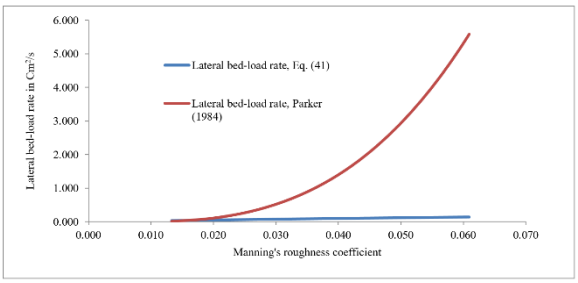

Fig. 4: The lateral bed-load transport by modified-Parker and Parker (1984) equation

Therefore, it could be concluded that Eq. (41) gives the best prediction (at least conceptually speaking) for the lateral bed-load transport rate and it can be used in sediment and morphological models. This equation although developed for fully developed flow conditions (uniform flow) could be used for non-uniform flow conditions in numerical models as it is a common practice to use equations (such as resistance and bed-load equations) developed under uniform flow (fully developed) conditions for non-uniform and gradually varied conditions.

It should be noted that the present approach is based on one-dimensional analysis in the vertical direction as done for the transverse velocity and transverse boundary shear. However, the developed equations herein could be used in another different dimension as seen when the developed transverse bed-slope equation was used along the stream-wise direction (s) through Eq. (54). Similarly, the developed equations were used in several analyses, Bridge (1977); Odgaard (1984; 1986a-b), concerned with the lateral direction, r, as in calculating the lateral depth and sediment grain sizes distributions. This means that the developed equations herein can be useful in analyses concerned with stream-wise and transverse directions.

Along the same lines as above, a quasi-nonlinear approach could be used in which mild curvature conditions ($r_c >> B$, where r_c is the center radius of curvature) are assumed. This leads to neglecting the terms that have the velocity combinations (u, v), (u, w), (v, w)); where u, v, and w are the main, lateral, and vertical velocity components, respectively. This process simplifies considerably the equations of motion, Chang (1992); Hafez (2024). The resulting equations contain the local flow depth and the local depth-averaged velocity which could be assumed to depend on the radial direction, r. Then integration of the resulting equations with respect to becomes possible when using relations for the lateral variations of $D(r)$ and $\overline{U}(r)$, i.e., assuming topographic steering condition which is addressed in Blanckaert (2010); Hafez (2023).

Table (5) shows the deviation angles for the resultant flow velocity, Eq. (48) and the resultant bed-load discharge, Eq. (49), derived from the resultant boundary shear deviation angle, Eq. (46), versus channel roughness. It can be seen that the deviation angles for the resultant flow velocity are the highest followed by that of the boundary shear then lastly comes the bed-load discharge with the common decreasing trend among the three angles versus increasing channel roughness. The deviation angles for the resultant velocities at low roughness values are comparable to Rozovskii (1957) such that: $(\delta_{vb}) \approx \arctan(11\ D/r) \approx 23.8°$. Table (5) shows also that at n = 0.01 (low roughness) the lateral bed-load discharge is about 6% of the longitudinal bed-load discharge while this ratio reduces to about 2% at n = 0.1 (high roughness). Eqs. (48-49) have an advantage over Eqs. (45 and 47), respectively in that no knowledge is required for the near-bed velocity or the longitudinal bed-load discharge because knowledge of them is a very challenging task. Comparing the results of predictions by Eqs. (45 and 48) for the resultant flow velocity deviation angle, the angles by Eq. (48) have a narrow range between 21.5 and 15.0° while the range by Eq. (45) is between 58.8 and 9.1°, Hafez (2024). However, both equations have an advantage over the relation: $Tan\ \delta_{vb} \approx 11\ \frac{D}{r}$ in including the roughness effects which definitely play an important role in all flow and sediment investigations. Both equations, Eqs. (45 and 48) could be used in equations such as by Bridge (1977) for the transverse bed slope and in the modified Parker equation for the bed-load deviation angle. Equation (41) (modified Parker equation) adopts the bed-load rate deviation angle by Eq. (48) which allowed the removal of the highly uncertain bed-load equation in the original Parker (1984) equation.

In summary, this study highlighted some weaknesses and deficiencies in past existing methods regarding the mechanics of sediment formation and transport in curved and alluvial meandering open channels. It shows the possibility of presenting improvements in past methods assumptions and equations and in the meantime utilizing their strength by adopting some past relations and combining them with newly developed equations as in the case of the developed transverse bed-load equation. It is recommended to investigate the applicability of methods of measurements of bed load such as (ISSDOTv2, The Integrated, Section Surface Difference Over Time, version 2), (McAlpin *et al*., 2023), to measure the transverse bed load rate.

Table 5: Deviation angles for the resultant bed shear, flow velocity, and bed-load discharge

Manning's roughness coefficient (n)	Resultant bed shear deviation angle from Eq. (46) in degrees	Resultant flow velocity deviation angle from Eq. (48) in degrees	Resultant bed-load rate deviation angle from Eq. (49) in degrees	$\tan \delta_\tau$ from Eq. (46) in radians	$\tan \delta_v$ from Eq. (48) in radians	$\tan \delta_{q_b}$ from Eq. (49) in radians
0.01	8.8	21.5	3.5	0.156	0.394	0.061
0.015	8.3	20.9	3.2	0.146	0.382	0.056
0.02	7.9	20.4	2.9	0.138	0.371	0.051
0.025	7.4	19.9	2.7	0.130	0.361	0.047
0.03	7.1	19.4	2.5	0.124	0.352	0.044
0.035	6.7	18.9	2.3	0.118	0.343	0.040
0.04	6.4	18.5	2.2	0.112	0.335	0.038
0.045	6.1	18.1	2.0	0.107	0.328	0.035
0.05	5.9	17.8	1.9	0.103	0.321	0.033
0.055	5.6	17.4	1.8	0.099	0.314	0.031
0.06	5.4	17.1	1.7	0.095	0.308	0.029
0.065	5.2	16.8	1.6	0.091	0.302	0.028
0.07	5.0	16.5	1.5	0.088	0.296	0.026
0.075	4.8	16.2	1.4	0.085	0.291	0.025
0.08	4.7	16.0	1.3	0.082	0.286	0.023
0.085	4.5	15.7	1.3	0.079	0.281	0.022
0.09	4.4	15.5	1.2	0.077	0.277	0.021
0.095	4.3	15.3	1.2	0.074	0.273	0.020
0.1	4.1	15.0	1.1	0.072	0.269	0.019

Conclusion

Expression for the bed-load discharge deviation angle is developed which allows distinction with the other two deviation angles of the flow velocity and the boundary shear. These expressions have the advantage of including the roughness and the main velocity in addition to including the water's average depth and the channel radius of curvature. The expression for the lateral boundary shear stress is used to improve the existing models for calculating transverse bed slope in a correct physical and conceptual form. The developed transverse bed slope compares very well with experimental and field data at Fall River and Muddy Creek, USA. Correction is made to the thickness of the bed-load layer in straight channels to fit curved channels. This enabled the improvement of the well-known equations by Bridge (1977); Ascanio and Kennedy (1983); Parker (1984) for the transverse bed slope by using improved expressions for the transverse boundary shear stress and the bed-load layer thickness in curved channels making their equations more physically correct.

An expression for the lateral bed-load transport is developed which has an advantage over that by Parker (1984) in balancing the lateral sediment movement upslope due to the secondary currents by the downslope movement of bed particles due to gravity. An equation is developed to predict the longitudinal bed-load transport in curved and alluvial meandering channels. Although the developed equations were derived under steady and fully developed flow conditions, they can be used in unsteady and non-uniform flow and sediment models in line with common practice when the unsteady and non-uniformity variations are gradually varied. In addition, the developed equations can be used in analyses concerned with the stream-wise and lateral directions.

Acknowledgment

The author would like to present his sincere gratitude and appreciation to anonymous reviewers for the very fruitful, informative, and important remarks, suggestions, and comments which really helped in the significant improving of this manuscript.

Funding Information

This study was conducted without any external funding.

Ethics

The author affirms that there are no known financial conflicts of interest or personal relationships that could have influenced the research presented in this study. Additionally, this study complies with ethical standards.

References

Ascanio, M. F., & Kennedy, J. F. (1983). Flow in alluvial-river curves. *Journal of Fluid Mechanics, 133*, 1–16. https://doi.org/10.1017/s0022112083001755

Blanckaert, K. (2010). Topographic steering, flow recirculation, velocity redistribution, and bed topography in sharp meander bends. *Water Resources Research, 46*(9). https://doi.org/10.1029/2009wr008303

Braithwaite, N. S. (2023). Regime Channel Bedload Transport Equation. *Journal of Hydraulic Engineering, 149*(3), 06022020. https://doi.org/10.1061/jhend8.hyeng-12983

Bridge, J. S. (1977). Flow, bed topography, grain size and sedimentary structure in open channel bends A three-dimensional model. *Earth Surface Processes*, *2*(4), 401–416. https://doi.org/10.1002/esp.3290020410

Bridge, J. S. (1992). A Revised Model for Water Flow, Sediment Transport, Bed Topography and Grain Size Sorting in Natural River Bends. *Water Resources Research*, *28*(4), 999–1013. https://doi.org/10.1029/91wr03088

Brunner, G. W. (2016). *HEC-RAS River Analysis System 2D Modeling User's Manual*. US Army Corps of Engineers—Hydrologic Engineering Center.

Chang, H. H. (1983). Energy expenditure in curved open channels. *Journal of Hydraulic Engineering*, *109*(7), 1012-1022. https://doi.org/10.1061/(ASCE)0733-9429(1983)109:7(1012)

Chang, H. H. (1984). Regular meander path model. *Journal of Hydraulic Engineering*, *110*(10), 1398-1411. https://doi.org/10.1061/(ASCE)0733-9429(1984)110:10(1398)

Chang, H. H. (1992). *Fluvial Processes in River Engineering* (1st Ed.). Krieger.

Da Silva, A. M. F. (2006). On why and how do rivers meander. *Journal of Hydraulic Research*, *44*(5), 579-590. https://doi.org/10.1080/00221686.2006.9521708

Dey, S., Mahato, R. K., & Ali, S. Z. (2023). Turbulent Shear Flow over a Downstream-Skewed Wavy Bed: Analytical Model Based on the RANS Equations with Boussinesq Approximation. *Journal of Hydraulic Engineering*, *149*(9), 04023028. https://doi.org/10.1061/jhend8.hyeng-13577

Dietrich, W. E., & Smith, J. D. (1983). Influence of the point bar on flow through curved channels. *Water Resources Research*, *19*(5), 1173–1192. https://doi.org/10.1029/wr019i005p01173

Dietrich, W. E., & Smith, J. D. (1984). Bed Load Transport in a River Meander. *Water Resources Research*, *20*(10), 1355–1380. https://doi.org/10.1029/wr020i010p01355

Engelund, F. (1974). Flow and Bed Topography in Channel Bends. *Journal of the Hydraulics Division*, *100*(11), 1631–1648. https://doi.org/10.1061/jyceaj.0004109

Falcon-Ascanio, M. A. (1979). *Analysis of Flow in Alluvial Channel Bends* (1st Ed.). The University of Iowa.

Ferreira da Silva, A. M., & Ebrahimi, M. (2017). Meandering Morphodynamics: Insights from Laboratory and Numerical Experiments and Beyond. *Journal of Hydraulic Engineering*, *143*(9), 03117005. https://doi.org/10.1061/(asce)hy.1943-7900.0001324

Hafez, Y. I. (2022). Excess energy theory for river curvature and meandering. *Journal of Hydrology*, *608*, 127604. https://doi.org/10.1016/j.jhydrol.2022.127604

Hafez, Y. I. (2023). Transverse energy loss slope in meandering channels. *Journal of Hydro-Environment Research*, *51*, 1–14. https://doi.org/10.1016/j.jher.2023.08.002

Hafez, Y. I. (2024). Transverse Velocity, Transverse Boundary Shear Stress and Flow Deviation in Meandering Open Channels. *American Journal of Environmental Sciences*, *20*(1), 1–21. https://doi.org/10.3844/ajessp.2024.1.21

Hasegawa, K. (1989). Universal Bank Erosion Coefficient for Meandering Rivers. *Journal of Hydraulic Engineering*, *115*(6), 744–765. https://doi.org/10.1061/(asce)0733-9429(1989)115:6(744)

He, L., Chen, D., Termini, D., Zhang, S., & Zhu, Z. (2021). Experiments on Longitudinal and Transverse Bedload Transport in Sine-Generated Meandering Channels. *Applied Sciences*, *11*(14), 6560. https://doi.org/10.3390/app11146560

Ikeda, S. (1982). Lateral Bed Load Transport on Side Slopes. *Journal of the Hydraulics Division*, *108*(11), 1369–1373. https://doi.org/10.1061/jyceaj.0005937

Karim, Md. F. (1981). *Computer-based Predictors for Sediment Discharge and Friction Factor of Alluvial Streams*. University of Iowa.

Kikkawa, H., Kitagawa, A., & Ikeda, S. (1976). Flow and Bed Topography in Curved Open Channels. *Journal of the Hydraulics Division*, *102*(9), 1327–1342. https://doi.org/10.1061/jyceaj.0004615

Lamb, M. P., Brun, F., & Fuller, B. M. (2017). Direct Measurements of Lift and Drag on Shallowly Submerged Cobbles in Steep Streams: Implications for Flow Resistance and Sediment Transport. *Water Resources Research*, *53*(9), 7607–7629. https://doi.org/10.1002/2017wr020883

McAlpin, T. O., Wren, D. G., Jones, K. E., Abraham, D. D., Kuhnle, R. A., & Willson, C. S. (2023). Uncertainty for the ISSDOTv2 Bedload Measurement Method. *Journal of Hydraulic Engineering*, *149*(9), 04023036. https://doi.org/10.1061/jhend8.hyeng-13505

Meyer-Peter, E., & Muller, R. (1948). Formulas for Bed-Load Transport. *In IAHSR 2nd Meeting, Stockholm, Appendix 2. IAHR*, 38–65.

Nunner, W. (1956). *Wärmeübergang und Druckabfall in rauhen Rohern*.

Odgaard, A. J. (1982). Bed Characteristics in Alluvial Channel Bends. *Journal of the Hydraulics Division*, *108*(11), 1268–1281. https://doi.org/10.1061/jyceaj.0005932

Odgaard, A. J. (1984). Grain-Size Distribution of River-Bed Armor Layers. *Journal of Hydraulic Engineering*, *110*(10), 1479–1484. https://doi.org/10.1061/(asce)0733-9429(1984)110:10(1479)

Odgaard, A. J. (1986a). Meander Flow Model. I: Development. *Journal of Hydraulic Engineering*, *112*(12), 1117–1135. https://doi.org/10.1061/(asce)0733-9429(1986)112:12(1117)

Odgaard, A. J. (1986b). Meander Flow Model. II: Applications. *Journal of Hydraulic Engineering*, *112*(12), 1137–1149. https://doi.org/10.1061/(asce)0733-9429(1986)112:12(1137)

Parker, G. (1984). Discussion of "Lateral Bed Load Transport on Side Slopes" by Syunsuke Ikeda (November, 1982). *Journal of Hydraulic Engineering*, *110*(2), 197–199. https://doi.org/10.1061/(asce)0733-9429(1984)110:2(197)

Perret, E., Camenen, B., Berni, C., El kadi Abderrezzak, K., & Renard, B. (2023). Uncertainties in Models Predicting Critical Bed Shear Stress of Cohesionless Particles. *Journal of Hydraulic Engineering*, *149*(4), 04023002. https://doi.org/10.1061/jhend8.hyeng-13101

Rozovskii, I. L. (1957). *Flow of Water in Bends of Open Channels* (1st Ed.). Akademy of Sciences of the Ukrainian SSR.

Schmeeckle, M. W., Nelson, J. M., & Shreve, R. L. (2007). Forces on Stationary Particles in Near-bed Turbulent Flows. *Journal of Geophysical Research: Earth Surface*, *112*(F2), 1–21. https://doi.org/10.1029/2006jf000536

Thorne, C. R., Rais, S., Zevenbergen, L. W., Bradley, J. B., & Julien, P. Y. (1983). *Measurement of Bend Flow Hydraulics on the Fall River at Low Stage*. WRFSL Rep.

Weiss, S. F., & Higdon, J. J. L. (2022). Dynamics of meandering rivers in finite-length channels: linear theory. *Journal of Fluid Mechanics*, *938*, A11. https://doi.org/10.1017/jfm.2022.131

Yeh, K., & Kennedy, J. F. (1993). Moment Model of Nonuniform Channel-Bend Flow. II: Erodible Beds. *Journal of Hydraulic Engineering*, *119*(7), 796–815. https://doi.org/10.1061/(asce)0733-9429(1993)119:7(796)

Yen, C., & Yen, B. C. (1971). Water Surface Configuration in Channel Bends. *Journal of the Hydraulics Division*, *97*(2), 303–321. https://doi.org/10.1061/jyceaj.0002872

Zhou, Y., & Tang, Q. (2022). Meandering Characteristics of the Yimin River in Hulun Buir Grassland, Inner Mongolia, China. *Remote Sensing*, *14*(11), 2696. https://doi.org/10.3390/rs14112696

Zimmerman, C., & Kennedy, J. F. (1978). Transverse Bed Slopes in Curved Alluvial Streams. *Journal of the Hydraulics Division*, *104*(1), 33–48. https://doi.org/10.1061/jyceaj.0004922

Zimmermann, C. (1974). *Sohlausbildung, Reibungsfaktoren, Und Sedimenttransport in Gleich-Förmig Gekrümmten Und Geraden Gerinnen*. Inst. Hydromech. University of Karlsruhe.